JOURNAL OF APPLIED POLYMER SCIENCE VOL. 10, PP. 361-374 (1966)

Role of Capillary End Correction in Flow Analysis of Molten Polyethylene

A. RAM and M. NARKIS, *Department of Chemical Engineering, Technion, Israel Institute of Technology, Haifa, Israel*

Synopsis

The role of the capillary end correction in flow analysis of molten low-density polyethylenes has been analyzed. In spite of limitations of accuracy a quantitative approach has been undertaken. The results are much more complicated than predicted by Bagley in his early reports. The elastic component of the end correction is controlled by shear stress and shear modulus. The latter is affected by the size of the subchain between entangles, M_e, and by the degree of long-chain branches. Both are eventually dependent on the length of the chain, i.e., its molecular weight. In addition shear stress and temperature affect the process of disentanglement. Capillary end correction increases with increasing molecular weight and shear stress and with decreasing temperature. The available analysis of branching is still in controversy, and therefore no numerical parameters are yet proposed. A consistent theory of the response of entanglement couplings to shear forces and temperature is evaluated.

Introduction

It is well known that geometry affects viscometric measurements in short capillaries.[1] The need of an end correction may be eliminated by using capillaries of high length-to-radius (L/R) ratio. However, on analyzing flow behavior of molten polymers in long capillaries, high pressures are involved which might significantly affect the viscosity of the melt.[2] Additional practical reasons dictate the use of relatively short capillaries in melt flow viscometers.

Bagley[3] published an empirical method of calculating flow curves, independent of the capillary geometry. This method has been successfully used in flow of polymer melts,[4-6] polymer solutions,[7] and other polymeric liquids.

The end correction appears in eq. (1):

$$\tau_w = \Delta P/\{2[(L/R) + N]\} \tag{1}$$

where τ_w is shear stress at the wall and N is a fictitious length (expressed as number of radii) which takes into account the additional pressure losses due to unsteady profile at the entrance (establishment of the boundary layer) and to the development of elastic potential energy in the melt. By measuring flow in a set of capillaries of the same radius but different lengths, the values of N at various shear rates are graphically obtained. In polymer

melts the correction term N depends mainly on shear conditions and varies usually in the range of 0–15.

Bagley[3] has shown the dependence of N on shear rate. His empirical corrections have been used by other researchers. Additional analyses of end correction are given in the literature.[9,10] The hydrodynamic aspect of pressure loss at the capillary entrance for inelastic liquids will be discussed in a separate article.

According to Philippoff and Gaskins,[11] the end correction N consists of two terms, a viscous component and an elastic one, as follows:

$$N = m_v + (S_R/2) = m_v + m_e \tag{2}$$

In eq. (2), m_v is the geometrical (Couette) end correction while S_R represents the recoverable elastic shear strain at the capillary wall. This last term appears whenever normal stresses exist.

Bagley[12,13] used eq. (2) in flow analysis of two polyethylenes, a linear and a branched one. He found a constant value of 2 or the viscous term m_v. By assuming the validity of Hooke's law in shear he showed a linear increase of N with shear stress, indicating significant higher values for the branched polymer.

Kishi[14] correlated values of S_R with the expansion of a polymer jet emerging from the capillary, both originated by the melt elasticity. He assumed constant values of 0.77 for m_v.

Schott[15] divided the end-correction N into three terms:

$$N = m_1 + (S_R/2) + m_2 \tag{3}$$

m_2 depends on the entrance angle to the capillary as well as on the temperature and shear conditions.

In our work we have tried to analyze the role of end correction in flow of various low-density polyethylenes at different temperatures. We found a strong dependence of the end correction on the type of polymer, its molecular weight, temperature, and shear stress.

Experimental

Six commercial low-density polyethylenes samples (A–F) have been tested, as shown in Table 1. The molecular weights were estimated according to Peticolas.[16] Viscosity at 150°C. was determined at shear rates of 0.5–10 sec.$^{-1}$ by using a modified melt indexer with a capillary of $L/R = 28$. (The standard ratio is 8.) The end correction N in this range of shear rate was found to be around 2. The Newtonian viscosity η_0 was calculated by using the relationship of Ferry,[17] which fitted our data very well:

$$1/\eta = (1/\eta_0) + B\tau_w \tag{4}$$

In the case of samples E and F the temperature of 150°C. was considered too low, so that their Newtonian viscosity was determined at higher temperatures and extrapolated to 150°C. by using a semilogarithmic dependence of viscosity on $1/T$.

The intrinsic viscosity was measured in *p*-xylene at 85°C. According to the literature,[18] the correlations are as follows:

$$[\eta]_{x,85°C.} = 1.28[\eta]_{\alpha\text{-CN},\,125°C.}^{1.04} \tag{5}$$

Intrinsic viscosity in α-chloronaphthalene (α-CN) is correlated to the molecular weight of linear polyethylene, by

$$[\eta]_{\alpha\text{-CN},\,125°C.} = 4 \times 10^{-4}\bar{M}_w^{0.68} \tag{6}$$

The method of Peticolas[16] consists of guessing the index of long branches $\bar{n}_w$ and obtaining $\bar{M}_w$ by trial and error by using eqs. (5), (6), (7), and (8).

$$\eta_{0,b} = 3 \times 10^{-12}\bar{M}_w^{3.4} \exp\left\{-2.35(\bar{n}_w/12)\right\} \tag{7}$$

$$\bar{n}_w = [\eta]_l/[\eta]_b \tag{8}$$

where the subscripts b and l denote branched and linear polymer, respectively. Both intrinsic viscosities $[\eta]$ refer to the same $\bar{M}_w$.

TABLE I

Type	Density, g./cc.	Melt flow index MFI	$[\eta]_x$ (85°C.)	$[\eta]_{\alpha-CN}$ (calc.)	η_0 (150°C.), poise	$\bar{n}_w$ index of branching	$\bar{M}_w$ (calc.)
A	0.915	19.9	0.73	0.58	20,500	1.06	50,000
B	0.918	6.4	0.87	0.69	70,500	1.15	71,000
C	0.921	1.85	0.88	0.695	234,000	1.4	100,000
D	0.920	2.0	0.83	0.66	500,000	1.8	127,000
E	0.917	0.68	0.86	0.685	585,000	1.8	135,000
F	0.924	0.3	1.02	0.805	1,870,000	1.9	186,000

Flow curves at shear rates of 30–7000 sec.$^{-1}$ were obtained by use of an Atkinson-Nancarrow rheometer[19] (Tensometer Ltd., England). This is a capillary melt viscometer consisting of nine fixed speeds and capable of work in the range of 15–400 atm. The instrument has been modified after Skinner[20] in order to improve the temperature reading as close to the die as possible. Temperature control was within ±0.5°C. Four capillaries having the same radius of 1 mm. and L/R ratios of 8.7, 22, 34.7, 45.8 were used. In each case values of pressure were plotted against L/R at same shear-rates and extrapolated to zero pressure.

$$P = 2\tau_w[(L/R) + N] \tag{9}$$

The shear stresses at the wall were obtained by the slope of the graphs. Shear rates (noncorrected) were directly calculated by using the speed of the piston and the geometry of the capillary die.

Theory

We are chiefly interested in the evaluation of the elastic component of the end correction, m_e. The latter may be better related to the pressure drop ΔP_e due to the gain of elastic energy by the melt. Thus:

$$m_e = \Delta P_e/2\tau_w \tag{10}$$

According to Philippoff and Gaskins[11] this pressure drop is identical to the normal stress at the capillary wall P_{11}:

$$\Delta P_e = P_{11} = \tau_w S_R \tag{11}$$

By assuming that the mean value of normal stress over the whole flow area should be preferred over the value at the wall, we tried to calculate the boundary values for a simple model. The model is a modified Maxwell fluid, in which the elastic element is represented by the shear modulus G and the viscous component is expressed by a general equation as suggested by Gee and Lyon[21]:

$$1/\eta = (1/\eta_0) + b\tau^n \tag{12}$$

Equation (12) coincides with eq. (4) when $n = 1$. It also approximates a power law when η_0 is relatively large, while Newtonian behavior is approached for low shear stresses.

If the local pressure drop is expressed by

$$\Delta P_e{}^1 = \tau S = \tau^2/G \tag{13}$$

then the total elastic energy which is continuously supplied to a unit volume of fluid as it enters the capillary is given by

$$\Delta P_e = \frac{1}{Q}\int_0^R 2\pi r u(\tau^2/G)dr \tag{14}$$

where Q is volumetric flow rate, u = local velocity, and

$$\tau = \tau_w(r/R) \tag{15}$$

where R is the radius of the capillary. Integrating eq. (14) and using eqs. (10) and (15) leads to eq. (16):

$$m_e = \frac{\tau_w}{4G}\,\frac{(1/6\eta_0) + [b\tau_w{}^n/(n+6)]}{(1/4\eta_0) + [b\tau_w{}^n/(n+4)]} \tag{16}$$

On taking the conditions, $1/6\eta_0 \gg [b\tau_w{}^n/(n+6)]$ and $(1/4\eta_0) \ll [b\tau_w{}^n/(n+4)]$, the boundaries of m_e will be restricted by the proper values of the exponent n:

$$[(n+4)/(n+6)](\tau_w/4G) \geq m_e \geq \tau_w/6G \tag{17}$$

Assuming that n varies between zero and infinity, the result will be:

$$\tau_w/4G \geq m_e \geq \tau_w/6G \tag{18}$$

The lower boundary has also been claimed by Kriegl.[10] It is assumed that the actual range for m_e is quite limited. The magnitude of m_e is thus mainly related to the values of shear stress and shear modulus.

$$m_e = \tau_w/aG \tag{18a}$$

The value of the shear modulus G has been derived by use of the well-known theory of rubber elasticity. One gets the following relationship,[22,23] which holds mainly for crosslinked rubbers:

$$G = \rho RT/M_c \tag{19}$$

ρ is the polymer density, and M_c is the subchain between points of crosslinking. Equation (19) has been corrected for the two loose ends of the chain which do not contribute to the elastic response of the network segments. This correction leads to the expression:

$$G = (\rho RT/M_c)[1 - 2(M_c/M)] \tag{20}$$

In eq. (20), M represents the molecular weight of the whole original chain prior to crosslinking. In our case of molten polyethylene, the use of eqs. (19) and (20) has been suggested on replacing M_c by M_e, i.e., the subchains between entanglement points.[24] The polyethylene chains are visualized as an entangled network which closely resembles a crosslinked structure, at least when the elastic character is analyzed. The second term in eq. (20) should also be modified in order to include branched chains which consist of several loose ends. Therefore, an equivalent expression for low-density polyethylene melt gives:

$$G = (\rho RT/M_e)[1 - B(M_e/M)] \tag{21}$$

where $B \geq 2$, and this takes into account the actual number of loose ends. The latter belong to the long branches only.[25] In the case of linear chains, $B = 2$.

The effects of molecular weight, temperature, and shear stress on the values of M_e are of utmost importance. Actually not much is known about the size of the subchains between points of entanglements, except for the idea that entanglements may slip and change their location along the chain due to external forces.

Further theoretical analysis will be presented after the discussion of the experimental data.

Results and Discussion

Experimental results of the end correction N show its dependence on shear conditions, temperature, and molecular weight for low-density polyethylene samples.

In Figures 1 and 2, N is plotted against rate of shear (uncorrected) $\dot{\gamma}_N$ at different temperatures. The curves are essentially linear on a semilog scale with a positive slope. Our data obey the relationship:

$$N = p + q \log \dot{\gamma}_N \tag{22}$$

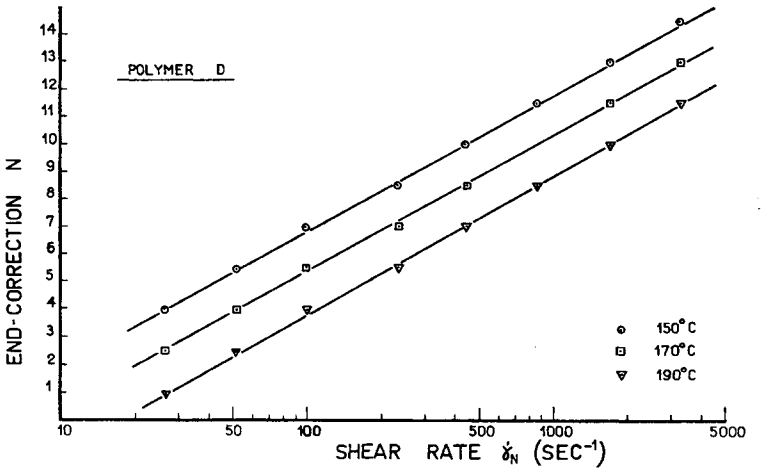

Fig. 1. Dependence of end correction on shear rate at various temperatures.

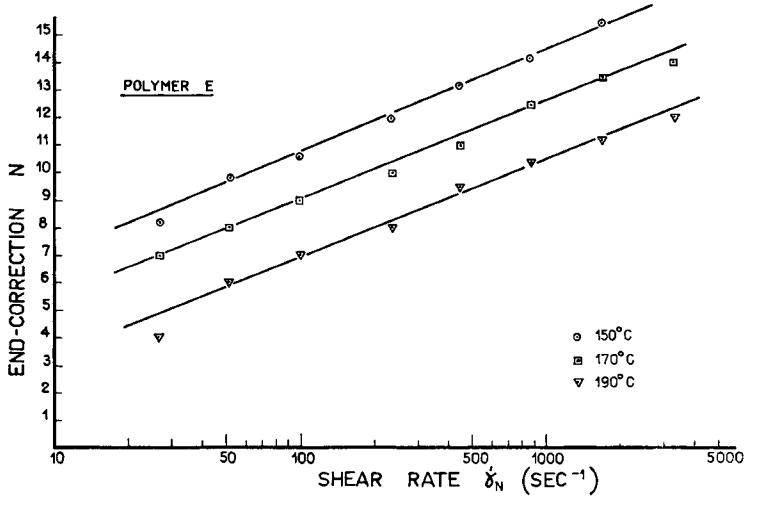

Fig. 2. Dependence of end correction on shear rate at various temperatures.

While the slope q is almost equal at three different temperatures, the coefficients p and hence the values of N decrease with temperature at the same shear rate. The reason for using $\dot{\gamma}_N$ instead of τ_w in these figures is due to the fact that $\dot{\gamma}_N$ is easily and independently calculated while the correct value of τ_w necessitates the use of the end correction. Equation (18a) should be modified by using the proper relationship between shear stress and rate of shear. If the Power law is used, the result becomes:

$$m_e = K(\dot{\gamma}_N)^{n'}/aG \tag{23}$$

K, like apparent viscosity, is temperature sensitive and decreases with increasing temperature. On the other hand, G is known from eq. (21) to

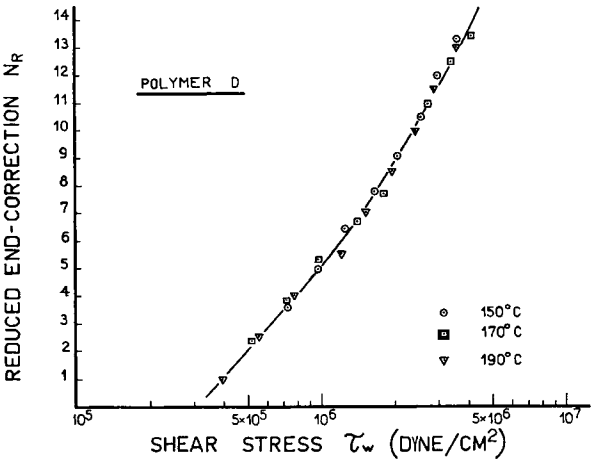

Fig. 3. Dependence of reduced end correction on shear stress.

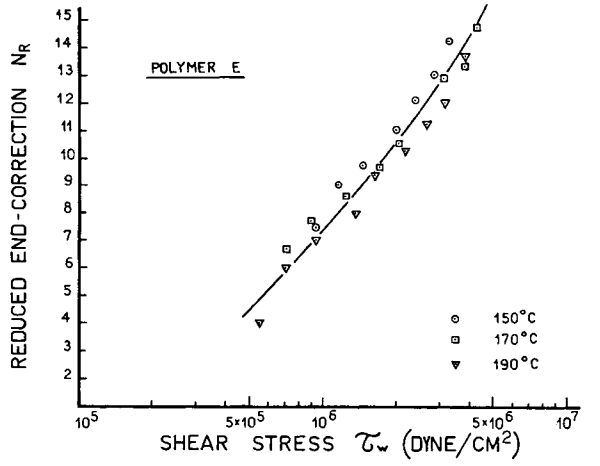

Fig. 4. Dependence of reduced end correction on shear stress.

increase with temperature. In this case both parameters K and G affect the lower values of m_e at higher temperatures. The effect of temperature could be neglected by using a method of superposition. A reduced value of N_R (to 190°C.) is defined as:

$$N_R = N(273 + T)/(273 + 190) \tag{24}$$

Such a linear displacement should hold for correlations of m_e with τ_w, where only G in eq. (18a) is temperature-dependent. However, the difference between m_e and N becomes negligible. Figures 3 and 4 show the relationship between N_R and τ_w. The curves are almost linear on a semilogarithmic scale, while according to eq. (18a) a straight line on rectangular coordinates is envisioned. This contradicts the findings of Bagley,[12]

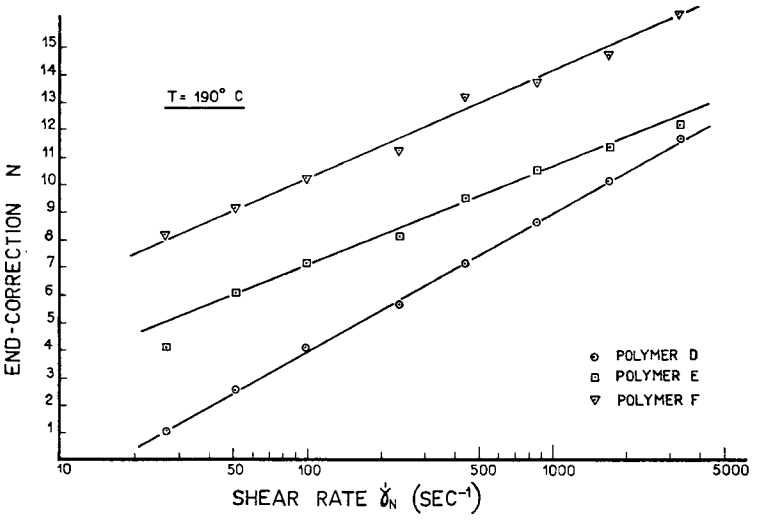

Fig. 5. Dependence of end correction on shear rate for various $\bar{M}_w$.

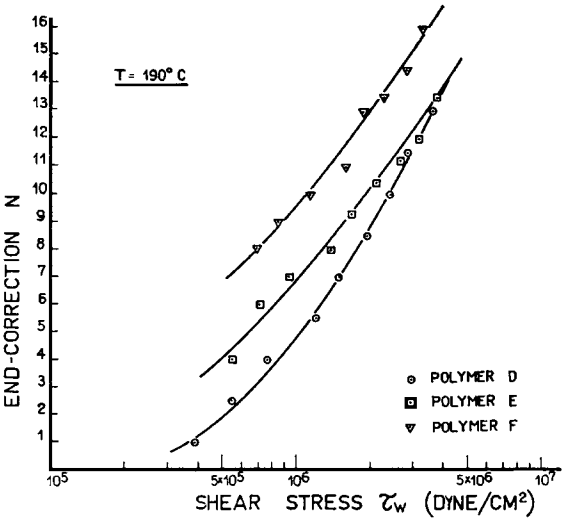

Fig. 6. Dependence of end correction on shear stress for various $\bar{M}_w$.

who found a linear dependence of N on τ_w for two low-density polyethylenes. In our case Hooke's law in shear is not obeyed, and we postulate that G is shear-dependent.

Another important variable is the molecular weight. In Figures 5 and 6 the effect of $\bar{M}_w$ on the curves of N versus $\dot{\gamma}_N$ or τ_w is clearly shown.

The temperature was kept at 190°C. and the values of N are significantly higher for higher molecular weights. As before, the correlation with $\dot{\gamma}_N$ is clearer than that with τ_w. Similar results are shown in Figures 7 and 8 at 150°C. However in Figure 8 the values for the three different $\bar{M}_w$

essentially coincide at the same shear stresses. Figure 9 shows the change of N with τ_w on a rectangular scale. As stated before no straight line is visualized. Moreover, the slopes of the curves decrease on increasing shear stress. The conclusion from Figure 9 might be that the shear modulus G will increase with shear stress. This dependence should be accounted for in eq. (21).

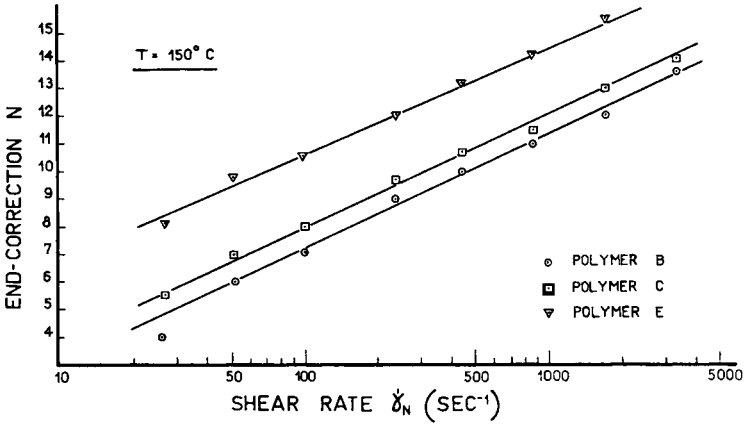

Fig. 7. Dependence of end correction on shear rate for various $\bar{M}_w$.

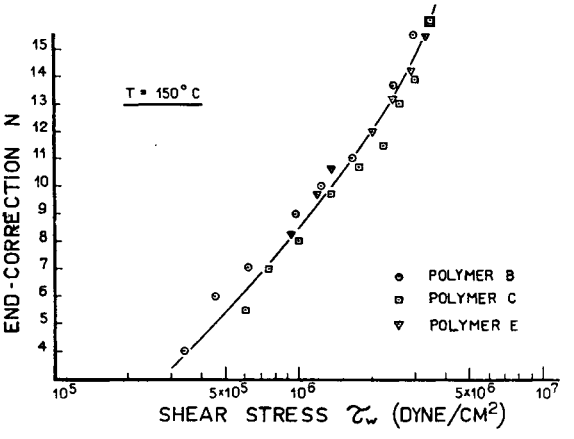

Fig. 8. Dependence of end correction on shear stress for various $\bar{M}_w$.

It is interesting to compare our results to those of Schott and Kaghan.[26] They also found the dependence of N on temperature, shear rate, and $\bar{M}_w$ in the same direction as ours. They also emphasize the small end correction for linear polyethylenes, resulting from higher entanglement frequency for the latter. It has been well accepted that branched chains are more compact and less able to entangle. From eq. (21) we notice that at constant temperature G is controlled by the values of M_e and B/M. A linear

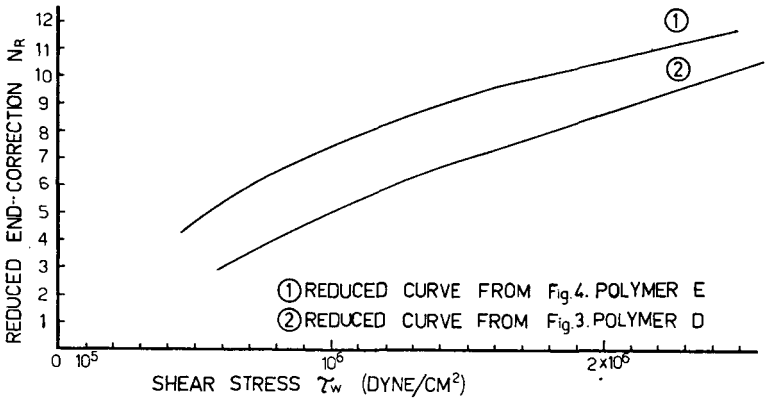

Fig. 9. Dependence of end correction on shear stress (linear coordinates).

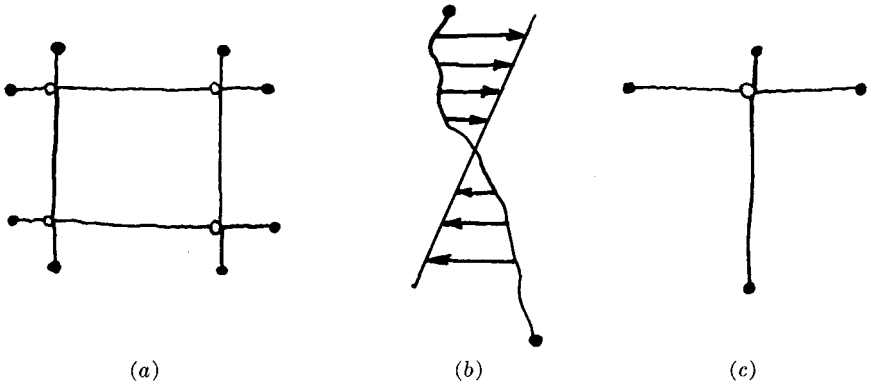

Fig. 10. (*a*) Unsheared; (*b*) velocity profile; (*c*) sheared.
● = end of chain. O = entanglement.

polyethylene has the smallest value for $B = 2$, and M_e is relatively smaller than that for a branched chain, so that G must be larger.

Johnson and Baer[8] got also higher end corrections for higher molecular weights.

A consistent picture which will explain our data is now represented. The elastic deformation is due to a network of entangles. The shortest chain that shows this effect is one that is tied by physical entanglements to two different ones. This may be shown by Figure 10*a*.

The effect of shear on flowing chains (Fig. 10*b*) will cause the entanglement points to slip towards the center. When each chain has only two coupling points, increasing shear will eventually unify them to the state shown in Figure 10*c*, which is no more considered as a network structure. The critical molecular weight (M_c) on the plot of η versus $\bar{M}_w$ which indicates the start of an entangled network should therefore increase at higher shear rates. In contradiction, Porter and Johnson[27] indicated a constant M_c, while the lines at increasing shear rates show progressively decreasing

slopes beyond the critical point. Schreiber et al.[28] found two distinctive M_c for their polyethylenes of a broad $\bar{M}_w$ range. The second M_c decreases with shear rate and represents the limit of Newtonian flow. Schreiber[29] postulates a third possibility, in which both the critical $\bar{M}_w$ and the slopes are shear-sensitive. The three models are shown in Figure 11.

Though Schreiber admits that the model shown in Figure 11*c* is most logical, he states that it has not yet been confirmed experimentally. We have, however, recently noticed such relationships for whole linear polyethylenes. Details about these findings will be published separately.

On increasing molecular weight, it is evident that more entanglement points will appear. Normally it is believed that the subchain between entangles, M_e, remains statistically constant at any chain length. The shearing forces will, however, cause slippage of the entanglement points.

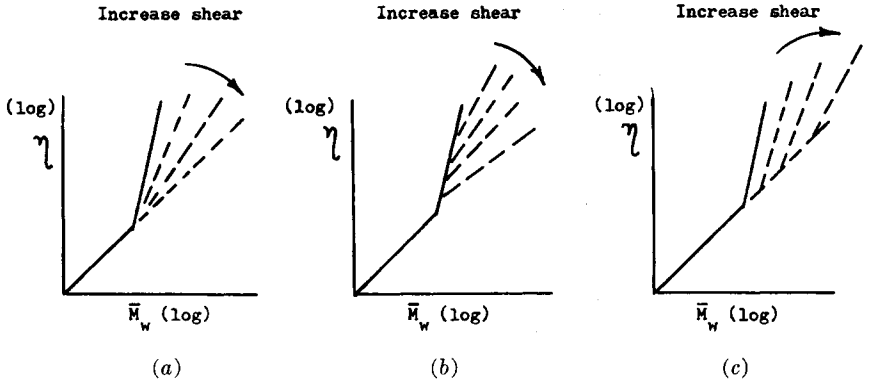

Fig. 11. Models of (*a*) Porter and Johnson,[27] (*b*) Schreiber et al.,[28] and (*c*) Schreiber.[29]

While total disentanglement is not possible for concentrated solutions or polymer melts, the size of the average subchain will eventually decrease. This reduction is more effective for the shorter chains and will be progressively less pronounced for the longer ones. Therefore higher shear will reduce M_e and thus higher values of G are obtained [by eq. (21)]. Such an increase of G with τ has been experimentally found for polyethylene by Benbow and Howells.[30] Similar increase of shear modulus with shear rate (in a limited range) has been confirmed by Vinogradov and Belkin.[31]

On increasing $\bar{M}_w$, the size of M_e becomes less affected by shear forces. The conclusion is that under identical shear conditions, larger molecules have larger average M_e. As we deal with branched chains, the value of B in eq. (21) and its dependence on $\bar{M}_w$ should be verified. As stated before, it is the long-chain branches that modify the rheological properties. The average number of long-chain branches per molecule has been calculated by Zimm and Stockmayer[32] by using the branching parameter g. By definition:

$$g = (S^2)_b/(S^2)_l = (R^2)_b/(R^2)_l \tag{25}$$

where S is the radius of gyration of the chain, R is the end-to-end distance, and b and l denote branched and linear polymer chains, respectively.

Equation (25) may be rewritten as:

$$g^{3/2} = [\eta]_b/[\eta]_l \tag{26}$$

$[\eta]_b$ $[\eta_l]$ are intrinsic viscosities.

Zimm and Kilb[33] claim that g is better correlated by:

$$g^{1/2} = [\eta]_b/[\eta]_l \tag{27}$$

Equation (27) suggests exceptionally high values for long-chain branches per molecule for our polyethylene samples. For the same reasons, Guillet[34] preferred to use eq. (26). The latter made a slight correction for the effect of short branches on g. They found approximate constant frequencies of branches on using eq. (26) but increasing frequencies with $\bar{M}_w$ when eq. (27) was adopted. The discrepancy between the various approaches is quite large, and an exact quantitative analysis may be unfortunately doubted. The dependence of the number of long branches on g is given in the literature.[35,36] We have calculated the number of branches per 1000 CH_2 groups (frequency) for our polyethylene samples. By use of either eq. (26) or (27) we have verified that the frequency of branching increases with $\bar{M}_w$. Therefore the group B/M in eq. (21) increases at higher $\bar{M}_w$, and this results in smaller values of G. We, therefore, postulate that the shear modulus decreases at higher molecular weights of branched polyethylenes. Higher frequency of long-chain branches for higher $\bar{M}_w$ was also predicted by Beasley[37] and verified by others.[38] In addition, Sperati et al.[25] showed that the shear modulus drops on increase of long-chain branching.

On using eq. (21) and calculating branching frequency according to eq. (26) and data from the literature, we arrive at a value of M_e in the vicinity of 15,000–20,000. These results are relatively 3–4 times the critical $\bar{M}_w$ (M_c) for polyethylene, but in line with recent publications of Schreiber, Rudin, and Bagley.[39] The effects of shear stress and temperature on M_e should not be underestimated.

The surprising behavior at 150°C. (as shown in Fig. 8) indicates that molecular weight does not affect the end correction dependence on τ_w at low temperatures. However, because of the marked effect of $\bar{M}_w$ on K in eq. (23), Figure 7 does show the role of $\bar{M}_w$ on a plot of N versus $\dot{\gamma}_N$. Porter and Johnson[40] and Tung[41] claim that the effectiveness of disentanglement increases at higher temperatures because of better mobility. That is the reason that at low temperatures branched polyethylenes show relatively higher frequencies of entanglement which resemble those of linear chains. We have also calculated data from Arai and Aoyama[42] that show that on a plot of end correction N versus τ_w, lines for different $\bar{M}_w$ coincide. Temperature should therefore also affect the value of the critical

$\bar{M}_w$ for entanglements. This is actually shown by Porter and Johnson,[43] where $\bar{M}_e$ increases at rising temperatures.

This work is partly based on the Sc.D. thesis of M. Narkis, to be submitted to the Department of Chemical Engineering, Israel Institute of Technology.

References

1. Ram, A., and A. Tamir, *Ind. Eng. Chem.*, **56**, 47 (1964).
2. Maxwell, B., and A. Jung, *Mod. Plastics*, **35**, 174 (1957).
3. Bagley, E. B., *J. Appl. Phys.*, **28**, 624 (1957).
4. Metzger, A. P., and R. S. Brodkey, *J. Appl. Polymer Sci.*, **7**, 399 (1963).
5. Ryder, L. B., *SPE J.*, **17**, 1305 (1961).
6. Eckert, R. E., *J. Appl. Polymer Sci.*, **7**, 1715 (1963).
7. Chinai, S. N., and W. C. Schneider, *J. Appl. Polymer Sci.*, **7**, 909 (1963).
8. Johnson, D. L., and Baer, E., *J. Appl. Polymer Sci.*, **7**, 1359 (1963).
9. Pezzin, G., *Materie Plastische Elastomeri*, August 1962.
10. Kriegl, H. J., *Österr. Chemiker Z.*, **4**, 115 (1962).
11. Philippoff, W., and F. H. Gaskins, *Trans. Soc. Rheol.*, **2**, 263 (1958).
12. Bagley, E. B., *J. Appl. Phys.*, **31**, 1126 (1960).
13. Bagley, E. B., *Trans. Soc. Rheol.*, **5**, 355 (1961).
14. Kishi, N., and H. Iizuka, *J. Polymer Sci.*, **B2**, 399 (1964).
15. Schott, H., *J. Polymer Sci.*, **A2**, 3791 (1964).
16. Peticolas, W. L., *J. Polymer Sci.*, **58**, 1405 (1962).
17. Ferry, J. D., *J. Am. Chem. Soc.*, **64**, 1330 (1947).
18. De La Cuesta, M. O., and F. W. Billmeyer, Jr., *J. Polymer Sci.*, **A1**, 1721 (1963).
19. Atkinson, E. B., and H. A. Nancarrow, *Proc. Intern. Rheol. Congr.*, Part I, 103 (1948).
20. Skinner, S. J., and W. Taylor, *Plastic Inst. Trans. J.*, **28**, 237 (1960).
21. Gee, R. E., and J. B. Lyon, *Ind. Eng. Chem.*, **49**, 956 (1957).
22. Tobolsky, A. V., *Properties and Structure of Polymers*, Wiley, New York, 1960.
23. Meares, P., *Polymers, Structure and Bulk Properties*, Van Nostrand, New York, 1965.
24. Markovitz, H., T. G Fox, and J. D. Ferry, *J. Phys. Chem.*, **66**, 1567 (1962).
25. Sperati, C. A., W. A. Franta, and H. W. Starkweather, *J. Am. Chem. Soc.*, **75**, 6127 (1953).
26. Schott, H., and W. S. Kaghan, *J. Appl. Polymer Sci.*, **5**, 175 (1961).
27. Porter, R. S., and J. F. Johnson, *J. Polymer Sci.*, **50**, 397 (1961).
28. Schreiber, H. P., E. B. Bagley, and D. C. West, *Polymer*, **4**, 355 (1963).
29. Schreiber, H. P., *Polymer*, **4**, 365 (1963).
30. Benbow, J. J., and E. R. Howells, *Polymer*, **2**, 429 (1961).
31. Vinogradov, G. V., and I. M. Belkin, *J. Polymer Sci.*, **A3**, 917 (1965).
32. Zimm, B. H., and W. H. Stockmayer, *J. Chem. Phys.*, **17**, 1301 (1949).
33. Zimm, B. H., and R. W. Kilb, *J. Polymer Sci.*, **37**, 19 (1959).
34. Guillet, J. E., *J. Polymer Sci.*, **A1**, 2869 (1963).
35. Mendelson, R. A., *J. Polymer Sci.*, **46**, 493 (1960).
36. Krause, S., and E. Cohn-Ginsberg, *J. Polymer Sci.*, **A2**, 1393 (1964).
37. Beasley, J. K., *J. Am. Chem. Soc.*, **75**, 6123 (1953).
38. Trementozzi, Q. A., *J. Polymer Sci.*, **22**, 187 (1956).
39. Schreiber, H. P., A. Rudin, and E. B. Bagley, *J. Appl. Polymer Sci.*, **9**, 887 (1965).
40. Porter, R. S., and J. F. Johnson, *Polymer*, **3**, 11 (1962).
41. Tung, L. H., *J. Polymer Sci.*, **46**, 409 (1960).
42. Arai, T., and H. Aoyama, *Trans. Soc. Rheol.*, **7**, 333 (1963).
43. Porter, R. S., and J. F. Johnson, *J. Appl. Phys.*, **32**, 2326 (1961).

Résumé

Le rôle de la correction de l'extrémité du cappilaire dans des analyses d'écoulement de polyéthylènes fondus de basse densité a été analysé: en dépit de limitations dues à l'imprécision une approche quantitative a été entreprise. Les résultats sont beaucoup plus compliqués que ceux prédits par Bagley dans ses rapports antérieurs. Le composant élastique de la correction est contrôlé par la tension de cisaillement et le mode de cisaillement; ce dernier est affecté par la grandeur de la partie des chaînes entre les enlacements successifs M_e et par le degré de ramifications à longue chaîne. Ces deux sont éventuellement dépendants de la longueur de la chaîne c.à.d. du poids moléculaire. En outre, la tension de cisaillement et la température affectent le processus de désenlacement. La correction pour l'extrémité du cappilaire croît avec augmentation du poids moléculaire et la tension de cisaillement et avec une diminution de température. L'analyse disponible du degré de ramification est encore contestée, et, de ce fait, aucun paramètre numérique n'est proposé jusqu'à présent. Une théorie consistante relative à la réponse de ces enchevêtrements aux forces de cisaillement et à la température est présentée.

Zusammenfassung

Die Rolle der Korrektur für das Kapillarenende bei der Fliessanalyse von geschmolzenen Polyäthylenen niedriger Dichte wurde untersucht. Trotz der durch die Versuchsgenauigkeit gegebenen Beschränkungen wurde eine quantitative Analyse unternommen. Die Ergebnisse sind viel komplizierter als nach den früheren Berichten von Bagley zu erwarten war. Die elastische Komponente der Endkorrektur wird durch Schubspannung und Schubmodul bestimmt. Letzterer wird durch die Grösse der Subketten zwischen Verschlingungsstellen, M_e, und durch den Grad der Langkettenverzweigung beeinflusst. Beide hängen von der Länge der Kette, d.h. ihrem Molekulargewicht ab. Ausserdem beeinflussen Schubspannung und Temperatur den Entschlingungsprozess. Die Korrektur für das Kapillarenende nimmt mit steigendem Molekulargewicht und steigender Schubspannung sowie mit fallender Temperatur zu. Bei der Verzweigungsanalyse bestehen noch Widersprüche, und daher werden noch keine numerischen Werte angegeben. Eine konsistente Theorie für das Verhalten einer Verschlingungskopplung gegen Schubkräfte und gegen die Temperatur wird aufgestellt.

Received July 30, 1965
Prod. No. 1273